터널과 지하공간, 한국암반역학회
Vol. 4, 1994, pp. 250~255

Tunnel and Site Investigations Using Seismic Tomography

Baek-Soo Suh[1], Hak-Soo Kim[2] and Byung-Doo Kwon[3]

탄성파 토모그래피를 이용한 터널탐사 및 부지조사

서백수 · 김학수 · 권병두

요 약

복잡한 지하구조인 지하터널과 핵폐기물 저장소 부지조사에 관한 자료해석을 위하여 지오토모그래피를 이용하였다. 지하터널의 조사는 지하저장소, 자원개발 및 군사적인 측면에서 많은 연구와 응용이 요구된다. 본 연구에서는 미육군이 현장에서 얻은 자료를 처리하고 이를 이론모형의 결과와 비교하였다. 또한 핵폐기물 부지 조사는 미국의 핵폐기물 저장소의 후보로 지정된 Yucca Mountain의 지질구조에 대한 이론모형계산을 행하였으며, Jaramillio(1993)가 모형실험치를 image 방법에 의하여 계산한 결과와 비교하였다. 탐사방법으로는 탄성파 시추공-시추공 방법과 VSP 방법을 사용하였다. 지오토모그래피의 기본이론은 터널과 지하공간 제3권 1호(1993)에서 설명되었다.

1. INTRODUCTION

Geotomography, which reconstructs underground structure, is very important task in recent geophysical and geotechnical investigations. In this study, two complex structures such as tunnel and hazardous waste repository site were shown to calculate geotomography.

Tunnel detection is greatly required in resources engineering and underground storage house, building. Cross-borehole seismic field data and theoretical model data were used to calculate geotomography.

Yucca Mountain geological section was used for theoretical modelling to apply this calculating method. This area is a candidate of hazardous waste repository site in U.S.A. Cross-borehole and VSP method were used in theoretical data aquisition.

* Received December 8, 1994
1) Full member, Prof., Kangwon National University
2) Ph. D, Seoul National University
3) Prof., Seoul National University

2. TUNNEL DETECTION

A target tunnel in the Idaho Mines located from 40 km west from Golden in Colorado State in the U.S.A. This field data were obtained by the U.S. Army and were processed by our research group. Next, another attempt was tried to get better field data. The result of field data processing was compared with that of theoretical data (Suh, 1993). Tunnel penetrates section BC and DE and advances to the north direction (Fig. 1). The spacings of borehole A and C, B and C, C and E were 75 ft, 34 ft and 52 ft, respectively. Data of each two boreholes were calculated. Fig. 2 shows the calculated geotomography of B and C boreholes field data. C and D boreholes geotomography and D and E boreholes geotomography were shown in Fig. 3 and 4. In these geotomography, tunnel was shown in the vicinity of actual tunnel position but shape of tunnel was deformed compared with the actual tunnel (Suh, 1993). The basic theory of geotomography

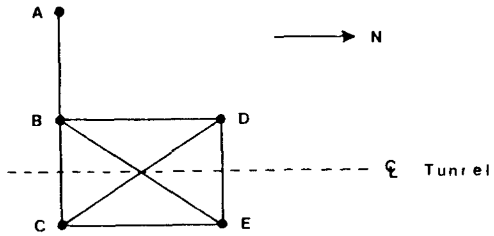

Fig. 1. Plan view of tunnel and borehole locations.

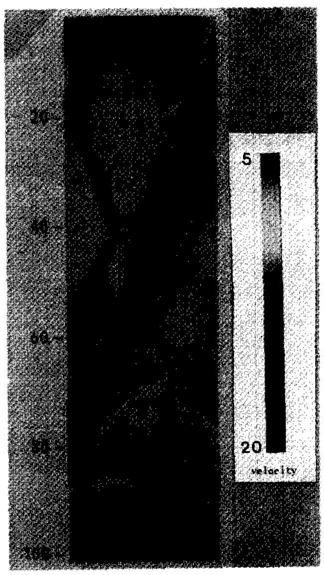

Fig. 2. Geotomography of B and C boreholes field data. The velocity (m/sec) of colorbar have to be multiplied by 1000 to those numbers.

was derived in previous paper (Suh, 1993) and the flowchart of calculating computer program was shown in Fig. 5.

Theoretical model was calculated to compare with the result of field data. The size of borehole B and C model was 34 ft in x-direction, 102 ft in z-direction. The distance and depth of boreholes in theoretical model were the same as those of field condition (Fig. 2).

The number of sources and receivers were 49 and 101, respectively. The mesh size of model was 1 ft and the number of meshes were 34 in x-direction and 102 in z-direction. The velocity of mother rock was supposed to 13,000 ft/sec and those of tunnel were 3,300 ft/sec (Fig. 6) assuming that tunnel was filled with water and 1,300 ft/sec (Fig. 7) assuming that tunnel was filled with air.

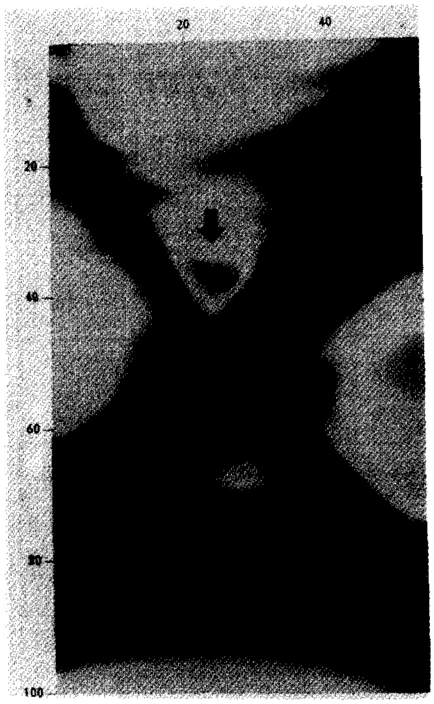

Fig. 3. Geotomography of C and D boreholes.

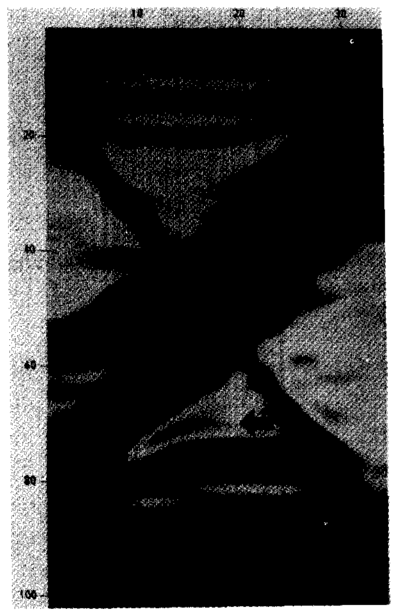

Fig. 4. Geotomography of D and E boreholes field data.

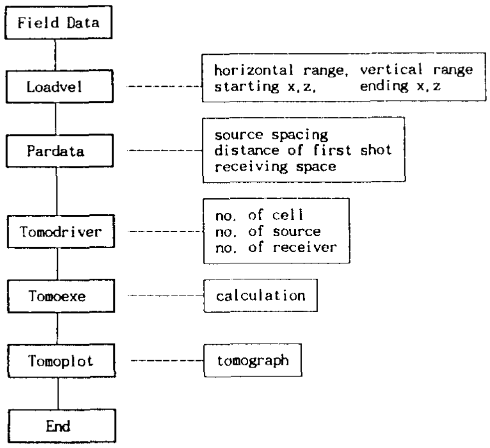

Fig. 5. The flow chart of computer program.

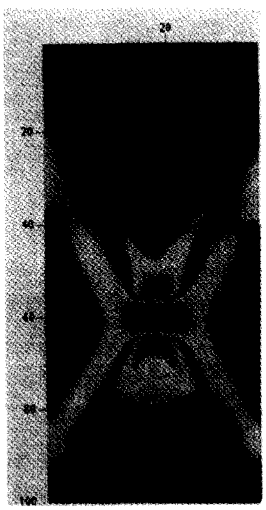

Fig. 6. Theoretical geotomography assuming that tunnel was filled with water.

To check the variety of tomography changing calculating iteration number, 4 times (1, 5, 10, 15) iterations were processed. The number of meshes were 34 in x-direction and 102 z-direction. The number of sources and receivers were 50, respectively. The velocity of mother rock was supposed to 10,000 ft/sec and that of tunnel was 3,300 ft/sec. The calculated results were shown in Fig. 8~11. When calculation was processed in 10 and 15 iteration number, large variety was not shown in calculated tomography (Fig. 10, 11). But it was 1 and 5 iteration number, large variety was shown in calculated geotomography (Fig. 8, 9).

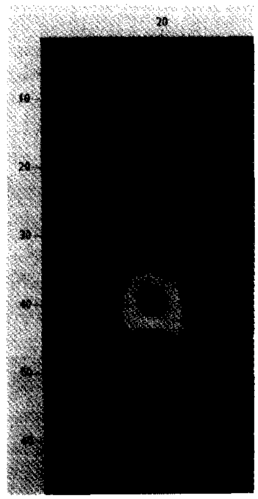

Fig. 7. Theoretical geotomography assuming that tunnel was filled with air.

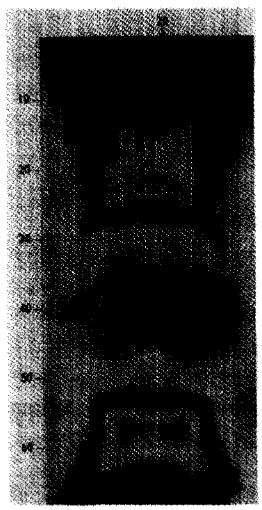

Fig. 8. Theoretical geotomography (Iteration number=1).

3. SITE INVESTIGATION

Above method was applied to investigate hazardous waste repository site. Theoretical modelling processed for the geological cross-section of the Yucca Mountain (Scott, 1984) was shown in Fig. 12. For the above geological structures a modelling experiment was proceeded with 24 sources at surface and 113 receivers in boreholes by Jaramillo (1993). The VSP (Vertical Seismic Profile) method was

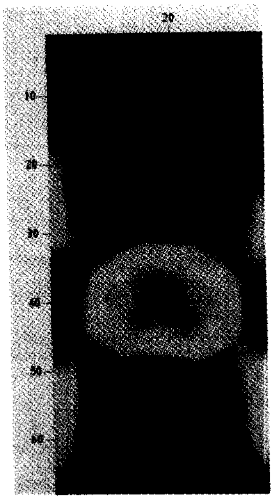

Fig. 9. Theoretical geotomography (Iteration number=5).

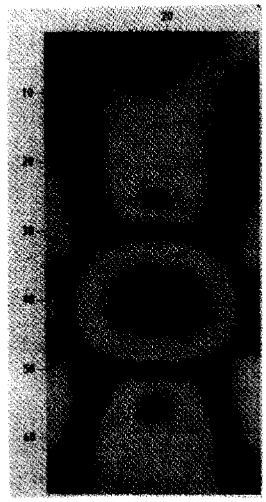

Fig. 11. Theoretical geotomography (Iteration number=15).

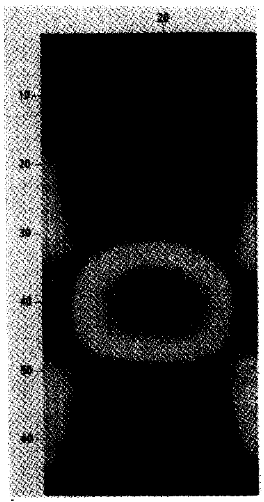

Fig. 10. Theoretical geotomography (Iteration number=10).

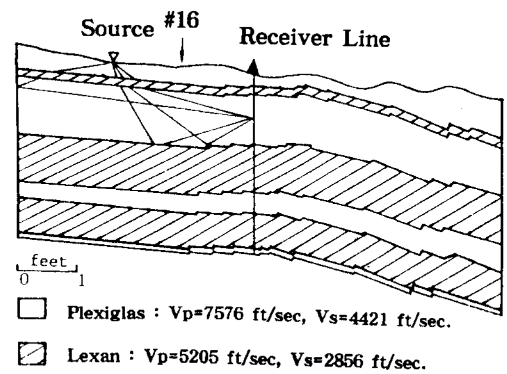

Fig. 12. Physical elastic Yucca Mt. model (Jaramillo, 1993). This model is based on Yucca Mt. by Scott (1984).

used to measure the seismic traveltime and the image method was applied to interpret the experimental data. For a model of variable velocity layered structure, plexiglass and lexan of which velocities were 7.756 ft/sec and 5.205 ft/sec, respectively were used.

Before data processing of complicated structures, preliminary simple fault model was conducted (Fig. 13). Sources were located at surface and receivers were located at 45 m point in vertically. Plexiglass and lexan were used for different layer velocities.

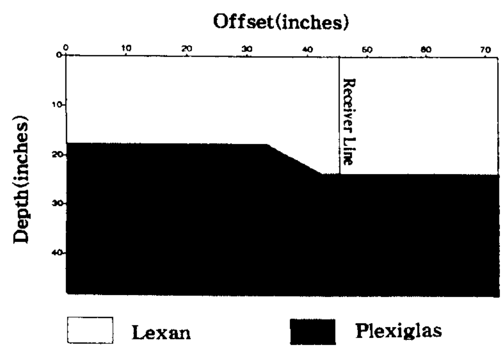

Fig. 13. Simple fault physical elastic model.

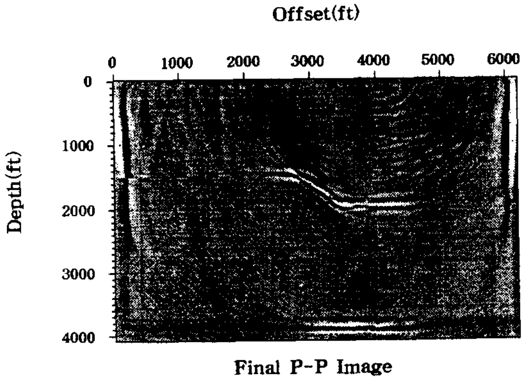

Fig. 14. The image method result of fault model (by Jaramillo).

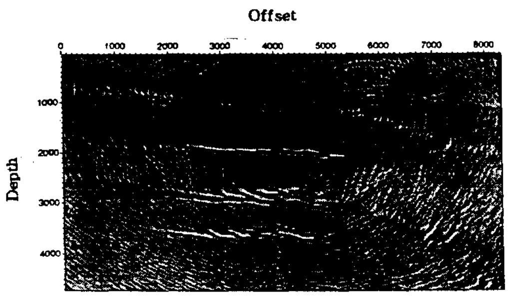

Fig. 15. The image method result of Yucca Mt. model (by Jaramillo).

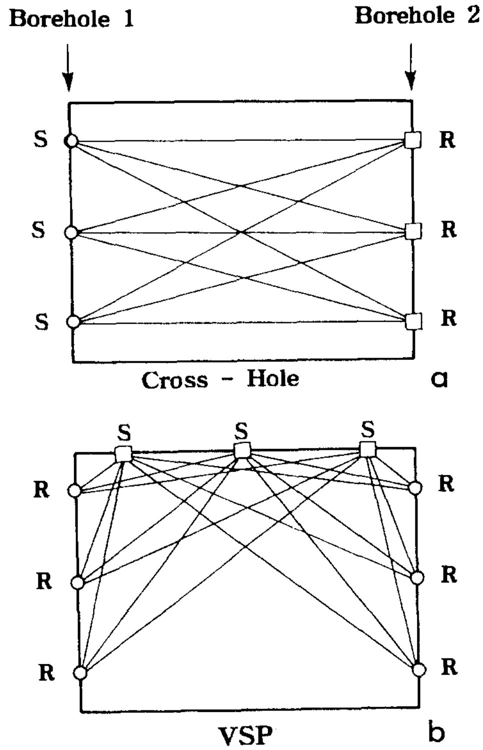

Fig. 16. Cross-borehole method and Vertical Seismic Profile (VSP) method.

The image method result of fault model processing experimental data by Jaramillo was shown in Fig. 14. The fault was shown clearly but thick lines at the edges, too. The image method result of Yucca Mountain processed by Jaramillo was shown in Fig. 15. Different layers could be classified by thick lines but it was very difficult to interpret for nonprofessionalist.

Theoretical geotomography was calculated in this simple model. Cross-borehole and VSP method (Fig. 16) were attempted in theoretical data aquisition.

The mesh size of model was 1 inch and the number of meshes were 45 in x-direction and 45 in z-direction. In cross-borehole method, 22 sources were arrayed every 2 inches in one borehole and 44 receivers were arrayed every 1 inch in another borehole. In VSP method, 22 sources were arrayed every 2 inches at surface and 22 receivers every 2 inches in one borehole, 44 receivers every 1 inch in another borehole.

The theoretical result of combination of VSP method and cross-borehole method was shown in Fig. 17 and fault was found at the result very clearly.

The theoretical calculation for Yucca Mountain modelling was conducted. Theoretical model size was 1/1000 of actual length of geological cross-section. Cross-borehole and VSP method were adapted to calculate the left part of geological section in Fig. 12. The model length of x- and z-direction was 50 ft. P wave velocities of layers were the same as those of experimental model. Mesh size of model was 1 ft×1 ft and the number of mesh in x- and z-direction was 50. 24 sources were arrayed every 2 ft at surface in and one borehole respectively, and 49 receivers were arrayed every 1 ft in another borehole. The geotomography of Yucca Mountain model was shown in Fig. 18 and was very similar with the actual geological cross-section.

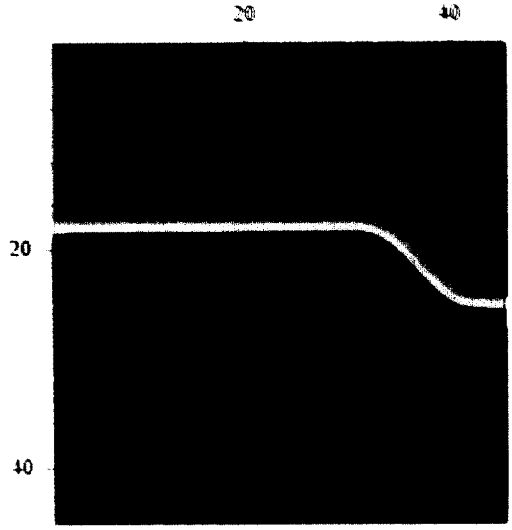

Fig. 17. Geotomography of simple fault model.

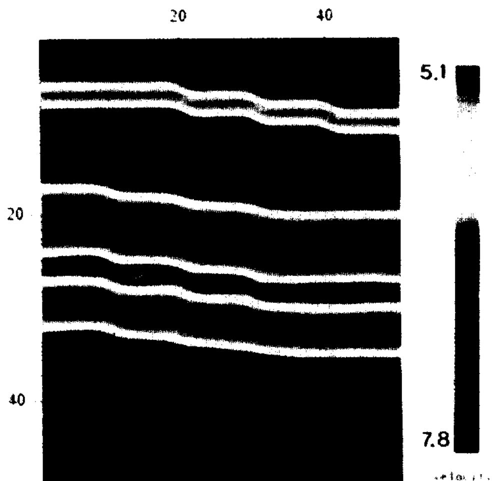

Fig. 18. Geotomography of Yucca Mt. geological cross-section model data.

4. CONCLUSION

1) A field data aquisition of exact first arrival time and plenty data is critical to get a better geotomography. And geophones have strong points in accuracy but have weak points in economy compared with hydrophone.

2) In tunnel and site investigations, it is recommended to perform both of VSP and cross-borehole method to get high resolution. And geotomography method is simple for non-professionals to interpret complex geological structures

5. ACKNOWLEDGEMENTS

This paper is a part of research which was supported by KOSEF GRANT (1994, Teuk Jung-94-1200-06-01-03). The authors would like to express our gratitude to KOSEF and related staffs.

REFERENCES

1) Cooke, D.A. and Schneider, W.A., Generalized linear inversion of reflection seismic data, Geophysics, Vol. 48, pp. 665-676 (1983).
2) Gersztenkorn, A. and Scales, J.A., Smoothing seismic tomograms with alpha-trimmed means, Geophysical Journal, Vol. 92, pp. 67-72 (1988).
3) Jaramillo, H.H., Computational and Physical modelling and Imaging of VSP data, M.S. Thesis 4302, Colorado School of Mines (1993).
4) Lines, L.R. and Treitel, S., A review of least squares inversion and its application to geophysics problem, Geophys. Prosp. Vol. 32, pp. 159-186 (1984).
5) McMechan, G.A., Seismic Tomography in boreholes, Geophy. Journal of the Royal Astr. Society, Vol. 74, pp. 601-612 (1982).
6) Peterson, R.G. and Paulsson, B.N., Applications of algebraic reconstruction techniques to crosshole seismic data, Geophysics, Vol. 50, pp. 1566-1580 (1985).
7) Pratt, R.G. and Worthington, M.H., The application of diffraction tomography to crosshole seismic data, Geophysics, Vol. 53, No. 10, pp. 1284-1294 (1988).
8) Scott, R.B., and Bonk, J., Preliminary geological map of Yucca Mountain, Nevada, with geological section, U.S.G.S. Open File Report pp. 84-494 (1984).
9) Suh, B.S. and Hyun, B.K., Tunnel detection using seismic geotomography, KRMS, Vol. 3, pp. 50-53 (1993).